Search for a Dark Leptophilic Scalar in e^+e^- Collisions

J. P. Lees,[1] V. Poireau,[1] V. Tisserand,[1] E. Grauges,[2] A. Palano,[3] G. Eigen,[4] D. N. Brown,[5] Yu. G. Kolomensky,[5] M. Fritsch,[6] H. Koch,[6] T. Schroeder,[6] R. Cheaib,[7b] C. Hearty,[7a,7b] T. S. Mattison,[7b] J. A. McKenna,[7b] R. Y. So,[7b] V. E. Blinov,[8a,8b,8c] A. R. Buzykaev,[8a] V. P. Druzhinin,[8a,8b] V. B. Golubev,[8a,8b] E. A. Kozyrev,[8a,8b] E. A. Kravchenko,[8a,8b] A. P. Onuchin,[8a,8b,8c] S. I. Serednyakov,[8a,8b] Yu. I. Skovpen,[8a,8b] E. P. Solodov,[8a,8b] K. Yu. Todyshev,[8a,8b] A. J. Lankford,[9] B. Dey,[10] J. W. Gary,[10] O. Long,[10] A. M. Eisner,[11] W. S. Lockman,[11] W. Panduro Vazquez,[11] D. S. Chao,[12] C. H. Cheng,[12] B. Echenard,[12] K. T. Flood,[12] D. G. Hitlin,[12] J. Kim,[12] Y. Li,[12] D. X. Lin,[12] T. S. Miyashita,[12] P. Ongmongkolkul,[12] J. Oyang,[12] F. C. Porter,[12] M. Röhrken,[12] Z. Huard,[13] B. T. Meadows,[13] B. G. Pushpawela,[13] M. D. Sokoloff,[13] L. Sun,[13,†] J. G. Smith,[14] S. R. Wagner,[14] D. Bernard,[15] M. Verderi,[15] D. Bettoni,[16a] C. Bozzi,[16a] R. Calabrese,[16a,16b] G. Cibinetto,[16a,16b] E. Fioravanti,[16a,16b] I. Garzia,[16a,16b] E. Luppi,[16a,16b] V. Santoro,[16a] A. Calcaterra,[17] R. de Sangro,[17] G. Finocchiaro,[17] S. Martellotti,[17] P. Patteri,[17] I. M. Peruzzi,[17] M. Piccolo,[17] M. Rotondo,[17] A. Zallo,[17] S. Passaggio,[18] C. Patrignani,[18,‡] B. J. Shuve,[19] H. M. Lacker,[20] B. Bhuyan,[21] U. Mallik,[22] C. Chen,[23] J. Cochran,[23] S. Prell,[23] A. V. Gritsan,[24] N. Arnaud,[25] M. Davier,[25] F. Le Diberder,[25] A. M. Lutz,[25] G. Wormser,[25] D. J. Lange,[26] D. M. Wright,[26] J. P. Coleman,[27] E. Gabathuler,[27,*] D. E. Hutchcroft,[27] D. J. Payne,[27] C. Touramanis,[27] A. J. Bevan,[28] F. Di Lodovico,[28,§] R. Sacco,[28] G. Cowan,[29] Sw. Banerjee,[30] D. N. Brown,[30] C. L. Davis,[30] A. G. Denig,[31] W. Gradl,[31] K. Griessinger,[31] A. Hafner,[31] K. R. Schubert,[31] R. J. Barlow,[32,∥] G. D. Lafferty,[32] R. Cenci,[33] A. Jawahery,[33] D. A. Roberts,[33] R. Cowan,[34] S. H. Robertson,[35a,35b] R. M. Seddon,[35b] N. Neri,[36a] F. Palombo,[36a,36b] L. Cremaldi,[37] R. Godang,[37,¶] D. J. Summers,[37] P. Taras,[38] G. De Nardo,[39] C. Sciacca,[39] G. Raven,[40] C. P. Jessop,[41] J. M. LoSecco,[41] K. Honscheid,[42] R. Kass,[42] A. Gaz,[43a] M. Margoni,[43a,43b] M. Posocco,[43a] G. Simi,[43a,43b] F. Simonetto,[43a,43b] R. Stroili,[43a,43b] S. Akar,[44] E. Ben-Haim,[44] M. Bomben,[44] G. R. Bonneaud,[44] G. Calderini,[44] J. Chauveau,[44] G. Marchiori,[44] J. Ocariz,[44] M. Biasini,[45a,45b] E. Manoni,[45a] A. Rossi,[45a] G. Batignani,[46a,46b] S. Bettarini,[46a,46b] M. Carpinelli,[46a,46b,**] G. Casarosa,[46a,46b] M. Chrzaszcz,[46a] F. Forti,[46a,46b] M. A. Giorgi,[46a,46b] A. Lusiani,[46a,46c] B. Oberhof,[46a,46b] E. Paoloni,[46a,46b] M. Rama,[46a] G. Rizzo,[46a,46b] J. J. Walsh,[46a] L. Zani,[46a,46b] A. J. S. Smith,[47] F. Anulli,[48a] R. Faccini,[48a,48b] F. Ferrarotto,[48a] F. Ferroni,[48a,††] A. Pilloni,[48a48b] G. Piredda,[48a,*] C. Bünger,[49] S. Dittrich,[49] O. Grünberg,[49] M. Heß,[49] T. Leddig,[49] C. Voß,[49] R. Waldi,[49] T. Adye,[50] F. F. Wilson,[50] S. Emery,[51] G. Vasseur,[51] D. Aston,[52] C. Cartaro,[52] M. R. Convery,[52] J. Dorfan,[52] W. Dunwoodie,[52] M. Ebert,[52] R. C. Field,[52] B. G. Fulsom,[52] M. T. Graham,[52] C. Hast,[52] W. R. Innes,[52,*] P. Kim,[52] D. W. G. S. Leith,[52,*] S. Luitz,[52] D. B. MacFarlane,[52] D. R. Muller,[52] H. Neal,[52] B. N. Ratcliff,[52] A. Roodman,[52] M. K. Sullivan,[52] J. Va'vra,[52] W. J. Wisniewski,[52] M. V. Purohit,[53] J. R. Wilson,[53] A. Randle-Conde,[54] S. J. Sekula,[54] H. Ahmed,[55] M. Bellis,[56] P. R. Burchat,[56] E. M. T. Puccio,[56] M. S. Alam,[57] J. A. Ernst,[57] R. Gorodeisky,[58] N. Guttman,[58] D. R. Peimer,[58] A. Soffer,[58] S. M. Spanier,[59] J. L. Ritchie,[60] R. F. Schwitters,[60] J. M. Izen,[61] X. C. Lou,[61] F. Bianchi,[62a,62b] F. De Mori,[62a,62b] A. Filippi,[62a] D. Gamba,[62a,62b] L. Lanceri,[63] L. Vitale,[63] F. Martinez-Vidal,[64] A. Oyanguren,[64] J. Albert,[65b] A. Beaulieu,[65b] F. U. Bernlochner,[65b] G. J. King,[65b] R. Kowalewski,[65b] T. Lueck,[65b] I. M. Nugent,[65b] J. M. Roney,[65b] R. J. Sobie,[65a,65b] N. Tasneem,[65b] T. J. Gershon,[66] P. F. Harrison,[66] T. E. Latham,[66] R. Prepost,[67] and S. L. Wu[67]

(*BABAR* Collaboration)

[1]*Laboratoire d'Annecy-le-Vieux de Physique des Particules (LAPP), Université de Savoie, CNRS/IN2P3, F-74941 Annecy-Le-Vieux, France*
[2]*Universitat de Barcelona, Facultat de Fisica, Departament ECM, E-08028 Barcelona, Spain*
[3]*INFN Sezione di Bari and Dipartimento di Fisica, Università di Bari, I-70126 Bari, Italy*
[4]*University of Bergen, Institute of Physics, N-5007 Bergen, Norway*
[5]*Lawrence Berkeley National Laboratory and University of California, Berkeley, California 94720, USA*
[6]*Ruhr Universität Bochum, Institut für Experimentalphysik 1, D-44780 Bochum, Germany*
[7a]*Institute of Particle Physics, Vancouver, British Columbia V6T 1Z1, Canada*
[7b]*University of British Columbia, Vancouver, British Columbia V6T 1Z1, Canada*
[8a]*Budker Institute of Nuclear Physics SB RAS, Novosibirsk 630090, Russia*
[8b]*Novosibirsk State University, Novosibirsk 630090, Russia*
[8c]*Novosibirsk State Technical University, Novosibirsk 630092, Russia*
[9]*University of California at Irvine, Irvine, California 92697, USA*
[10]*University of California at Riverside, Riverside, California 92521, USA*
[11]*University of California at Santa Cruz, Institute for Particle Physics, Santa Cruz, California 95064, USA*

[12]California Institute of Technology, Pasadena, California 91125, USA
[13]University of Cincinnati, Cincinnati, Ohio 45221, USA
[14]University of Colorado, Boulder, Colorado 80309, USA
[15]Laboratoire Leprince-Ringuet, Ecole Polytechnique, CNRS/IN2P3, F-91128 Palaiseau, France
[16a]INFN Sezione di Ferrara, I-44122 Ferrara, Italy
[16b]Dipartimento di Fisica e Scienze della Terra, Università di Ferrara, I-44122 Ferrara, Italy
[17]INFN Laboratori Nazionali di Frascati, I-00044 Frascati, Italy
[18]INFN Sezione di Genova, I-16146 Genova, Italy
[19]Harvey Mudd College, Claremont, California 91711, USA
[20]Humboldt-Universität zu Berlin, Institut für Physik, D-12489 Berlin, Germany
[21]Indian Institute of Technology Guwahati, Guwahati, Assam 781 039, India
[22]University of Iowa, Iowa City, Iowa 52242, USA
[23]Iowa State University, Ames, Iowa 50011, USA
[24]Johns Hopkins University, Baltimore, Maryland 21218, USA
[25]Université Paris-Saclay, CNRS/IN2P3, IJCLab, F-91405 Orsay, France
[26]Lawrence Livermore National Laboratory, Livermore, California 94550, USA
[27]University of Liverpool, Liverpool L69 7ZE, United Kingdom
[28]Queen Mary, University of London, London E1 4NS, United Kingdom
[29]University of London, Royal Holloway and Bedford New College, Egham, Surrey TW20 0EX, United Kingdom
[30]University of Louisville, Louisville, Kentucky 40292, USA
[31]Johannes Gutenberg-Universität Mainz, Institut für Kernphysik, D-55099 Mainz, Germany
[32]University of Manchester, Manchester M13 9PL, United Kingdom
[33]University of Maryland, College Park, Maryland 20742, USA
[34]Massachusetts Institute of Technology, Laboratory for Nuclear Science, Cambridge, Massachusetts 02139, USA
[35a]Institute of Particle Physics, Montréal, Québec H3A 2T8, Canada
[35b]McGill University, Montréal, Québec H3A 2T8, Canada
[36a]INFN Sezione di Milano, I-20133 Milano, Italy
[36b]Dipartimento di Fisica, Università di Milano, I-20133 Milano, Italy
[37]University of Mississippi, University, Mississippi 38677, USA
[38]Université de Montréal, Physique des Particules, Montréal, Québec H3C 3J7, Canada
[39]INFN Sezione di Napoli and Dipartimento di Scienze Fisiche, Università di Napoli Federico II, I-80126 Napoli, Italy
[40]NIKHEF, National Institute for Nuclear Physics and High Energy Physics, NL-1009 DB Amsterdam, Netherlands
[41]University of Notre Dame, Notre Dame, Indiana 46556, USA
[42]Ohio State University, Columbus, Ohio 43210, USA
[43a]INFN Sezione di Padova, I-35131 Padova, Italy
[43b]Dipartimento di Fisica, Università di Padova, I-35131 Padova, Italy
[44]Laboratoire de Physique Nucléaire et de Hautes Energies, Sorbonne Université, Paris Diderot Sorbonne Paris Cité, CNRS/IN2P3, F-75252 Paris, France
[45a]INFN Sezione di Perugia, I-06123 Perugia, Italy
[45b]Dipartimento di Fisica, Università di Perugia, I-06123 Perugia, Italy
[46a]INFN Sezione di Pisa, I-56127 Pisa, Italy
[46b]Dipartimento di Fisica, Università di Pisa, I-56127 Pisa, Italy
[46c]Scuola Normale Superiore di Pisa, I-56127 Pisa, Italy
[47]Princeton University, Princeton, New Jersey 08544, USA
[48a]INFN Sezione di Roma, I-00185 Roma, Italy
[48b]Dipartimento di Fisica, Università di Roma La Sapienza, I-00185 Roma, Italy
[49]Universität Rostock, D-18051 Rostock, Germany
[50]Rutherford Appleton Laboratory, Chilton, Didcot, Oxon OX11 0QX, United Kingdom
[51]IRFU, CEA, Université Paris-Saclay, F-91191 Gif-sur-Yvette, France
[52]SLAC National Accelerator Laboratory, Stanford, California 94309, USA
[53]University of South Carolina, Columbia, South Carolina 29208, USA
[54]Southern Methodist University, Dallas, Texas 75275, USA
[55]St. Francis Xavier University, Antigonish, Nova Scotia B2G 2W5, Canada
[56]Stanford University, Stanford, California 94305, USA
[57]State University of New York, Albany, New York 12222, USA
[58]Tel Aviv University, School of Physics and Astronomy, Tel Aviv 69978, Israel
[59]University of Tennessee, Knoxville, Tennessee 37996, USA
[60]University of Texas at Austin, Austin, Texas 78712, USA
[61]University of Texas at Dallas, Richardson, Texas 75083, USA

[62a]INFN Sezione di Torino, I-10125 Torino, Italy
[62b]Dipartimento di Fisica, Università di Torino, I-10125 Torino, Italy
[63]INFN Sezione di Trieste and Dipartimento di Fisica, Università di Trieste, I-34127 Trieste, Italy
[64]IFIC, Universitat de Valencia-CSIC, E-46071 Valencia, Spain
[65a]Institute of Particle Physics, Victoria, British Columbia, Canada V8W 3P6
[65b]University of Victoria, Victoria, British Columbia, Canada V8W 3P6
[66]Department of Physics, University of Warwick, Coventry CV4 7AL, United Kingdom
[67]University of Wisconsin, Madison, Wisconsin 53706, USA

(Received 6 May 2020; revised 17 September 2020; accepted 18 September 2020; published 28 October 2020)

Many scenarios of physics beyond the standard model predict the existence of new gauge singlets, which might be substantially lighter than the weak scale. The experimental constraints on additional scalars with masses in the MeV to GeV range could be significantly weakened if they interact predominantly with leptons rather than quarks. At an e^+e^- collider, such a leptophilic scalar (ϕ_L) would be produced predominantly through radiation from a τ lepton. We report herein a search for $e^+e^- \to \tau^+\tau^-\phi_L$, $\phi_L \to \ell^+\ell^-$ ($\ell = e, \mu$) using data collected by the *BABAR* experiment at SLAC. No significant signal is observed, and we set limits on the ϕ_L coupling to leptons in the range $0.04 < m_{\phi_L} < 7.0$ GeV. These bounds significantly improve upon the current constraints, excluding almost entirely the parameter space favored by the observed discrepancy in the muon anomalous magnetic moment below 4 GeV at 90% confidence level.

DOI: 10.1103/PhysRevLett.125.181801

Many theories beyond the standard model (SM) predict the existence of additional scalars, and discovering or constraining their existence might shed light on the physics of electroweak symmetry breaking and the Higgs sector (e.g., see Ref. [1]). Some of these particles may be substantially lighter than the weak scale, notably in the next-to-minimal supersymmetric standard model [2], but also in more generic singlet-extended sectors [3,4]. In the MeV–GeV range, new scalars could mediate interactions between the SM and dark matter, as well as account for the discrepancy in the observed value of the muon anomalous magnetic dipole moment [5–7].

The possible coupling of a new scalar ϕ_L to SM particles is constrained by SM gauge invariance. In the simplest case, the mixing between the scalar and the SM Higgs boson gives rise to couplings proportional to SM fermion masses. Because the new scalar couples predominantly to heavy-flavor quarks, this minimal scenario is strongly constrained by searches for rare flavor-changing neutral current decays of mesons, such as $B \to K\phi$ and $K \to \pi\phi$ [8]. However, these bounds are evaded if the coupling of the scalar to quarks is suppressed and the scalar interacts preferentially with heavy-flavor leptons [3,4,9,10]. We refer to such a particle as a leptophilic scalar, ϕ_L. Its interaction Lagrangian with leptons can be described by

$$\mathcal{L} = -\xi \sum_{\ell=e,\mu,\tau} \frac{m_\ell}{v} \bar{\ell}\phi_L \ell,$$

where ξ denotes the flavor-independent coupling strength to leptons and $v = 246$ GeV is the SM Higgs vacuum expectation value [11]. Model independent constraints relying exclusively on the coupling to leptons are derived from a *BABAR* search for a muonic dark force [12] and beam dump experiments [13,14]. A large fraction of the parameter space, including the region favored by the measurement of the muon anomalous magnetic moment, is still unexplored [3,9,10]. Examples of model dependent bounds from B and h decays for a specific UV completion of the theory can be found in Ref. [3].

The large sample of $\tau^+\tau^-$ pairs collected by *BABAR* offers a clean environment to study model independent ϕ_L production via final-state radiation in $e^+e^- \to \tau^+\tau^-\phi_L$. The mass proportionality of the coupling, in particular the feeble interaction with electrons, dictates the experimental signature. For $2m_e < m_{\phi_L} < 2m_\mu$, the scalar decays predominantly into electrons, leading to displaced vertices for sufficiently small values of the coupling. Prompt decays into a pair of muons (taus) dominate when $2m_\mu \le m_{\phi_L} < 2m_\tau$ ($2m_\tau < m_{\phi_L}$).

We report herein the first search for a leptophilic scalar in the reaction $e^+e^- \to \tau^+\tau^-\phi_L$, $\phi_L \to \ell^+\ell^-$ ($\ell = e, \mu$) for $0.04 < m_{\phi_L} < 7.0$ GeV. The cross section for $m_{\phi_L} < 2m_\mu$ is measured separately for ϕ_L lifetimes corresponding to $c\tau_{\phi L}$ values of 0, 1, 10, and 100 mm. Above the dimuon threshold, we determine the cross section for prompt $\phi_L \to \mu^+\mu^-$ decays. In all cases, the ϕ_L width is much smaller than the detector resolution, and the signal can be identified as a narrow peak in the dilepton invariant mass.

The search is based on 514 fb^{-1} of data collected at the $\Upsilon(2S)$, $\Upsilon(3S)$, $\Upsilon(4S)$ resonances and their vicinities [15] by the *BABAR* experiment at the SLAC PEP-II e^+e^- collider. The *BABAR* detector is described in detail elsewhere [16,17]. A sample corresponding to about 5% of the data, called the optimization sample, is used to optimize the search strategy and is subsequently discarded. The remaining data are examined only once the analysis procedure has been finalized.

Signal Monte Carlo (MC) samples with prompt decays are simulated for 36 different ϕ_L mass hypotheses by the MADGRAPH event generator [18] and showered using PYTHIA8 [19], including final-state radiation. For $m_{\phi_L} < 0.3$ GeV, events with $c\tau_{\phi L}$ values up to 300 mm are also generated. We simulate the following reactions to study the background: $e^+e^- \to e^+e^-(\gamma)$ (BHWIDE [20]), $e^+e^- \to \mu^+\mu^-(\gamma)$ and $e^+e^- \to \tau^+\tau^-(\gamma)$ (KK with the TAUOLA library [21,22]), $e^+e^- \to q\bar{q}$ with $q = u, d, s, c$ (Jetset [23]), and $e^+e^- \to B\bar{B}$ and generic $e^+e^- \to \Upsilon(2S, 3S)$ decays (EvtGen [24]). The resonance production $e^+e^- \to \gamma\psi(2S)$, $\psi(2S) \to \pi^+\pi^- J/\psi$, $J/\psi \to \mu^+\mu^-$ is simulated with EvtGen using a structure function technique [25,26]. The detector acceptance and reconstruction efficiencies are estimated with a simulation based on GEANT4 [27].

We select events containing exactly four charged tracks with zero net charge, focusing on τ lepton decays to single tracks and any number of neutral particles. The $\phi_L \to \ell^+\ell^-$ candidates are formed by combining two opposite-sign tracks identified as an electron or muon pair by particle identification (PID) algorithms [12,16]. We do not attempt to select a single ϕ_L candidate per event, but simply consider all possible combinations. Radiative Bhabha and dimuon events in which the photon converts to an e^+e^- pair are suppressed by rejecting events with a total visible mass greater than 9 GeV. We further veto $e^+e^- \to e^+e^-e^+e^-$ events by requiring the cosine of the angle between the momentum of the ϕ_L candidate and that of the nearest track to be less than 0.98, the missing momentum against all tracks and neutral particles to be greater than 300 MeV, and that there be three or less tracks identified as electrons. We perform a kinematic fit to the selected ϕ_L candidates, constraining the two tracks to originate from the same point in space. The dimuon production vertex is required to be compatible with the beam interaction region, while we only constrain the momentum vector of the e^+e^- pair to point back to the beam interaction region since the dielectron vertex can be substantially displaced. We select dielectron (dimuon) combinations with a value of the χ^2 per degree of freedom of the fit, $\chi^2/\mathrm{n.d.f.}$, less than 3 (12).

A multivariate selection based on boosted decision trees (BDT) further improves the signal purity [28]. The BDTs include variables capturing the typical τ and ϕ_L decay characteristics: a well-reconstructed $\ell^+\ell^-$ vertex, either prompt or displaced; missing energy and momentum due to neutrino emission; relatively large track momenta; low neutral particle multiplicity; and two or more tracks identified as electrons or muons. A few variables are also targeted at specific backgrounds, such as $\psi(2S) \to \pi^+\pi^- J/\psi, J/\psi \to \mu^+\mu^-$ production in initial-state radiation (ISR) events. The ϕ_L mass is specifically excluded to limit potential bias in the classifier. A full description of these variables can be found in the Supplemental Material [29]. We train a separate BDT for each of the different final states and $c\tau_{\phi L}$ values with signal events modeled using a flat m_{ϕ_L} distribution and background events modeled using the optimization sample data.

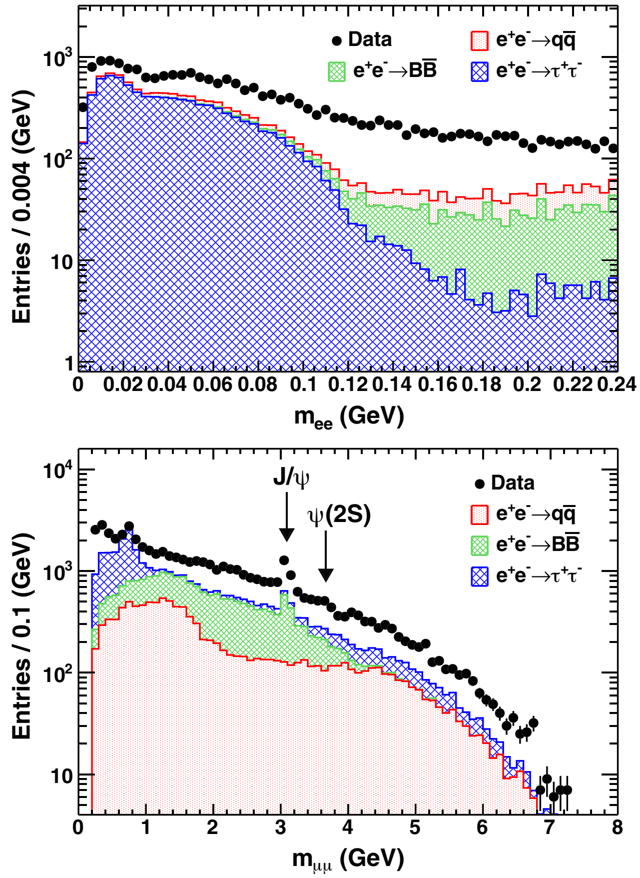

FIG. 1. The distribution of (top) the dielectron invariant mass and (bottom) the dimuon invariant mass for prompt decays, together with simulated predictions for the indicated processes normalized to the integrated luminosity of the data (stacked histograms).

The final selection of ϕ_L candidates for each lifetime selection and decay channel is made by applying a mass-dependent criterion on the corresponding BDT score that maximizes signal sensitivity. The distributions of the resulting dielectron and dimuon masses for prompt decays are shown in Fig. 1, and spectra for other lifetimes for $\phi_L \to e^+e^-$ decays are shown in Fig. 2, together with the dominant background components among the set of simulated MC samples. The differences between the data and summed-MC distributions are mainly due to processes that

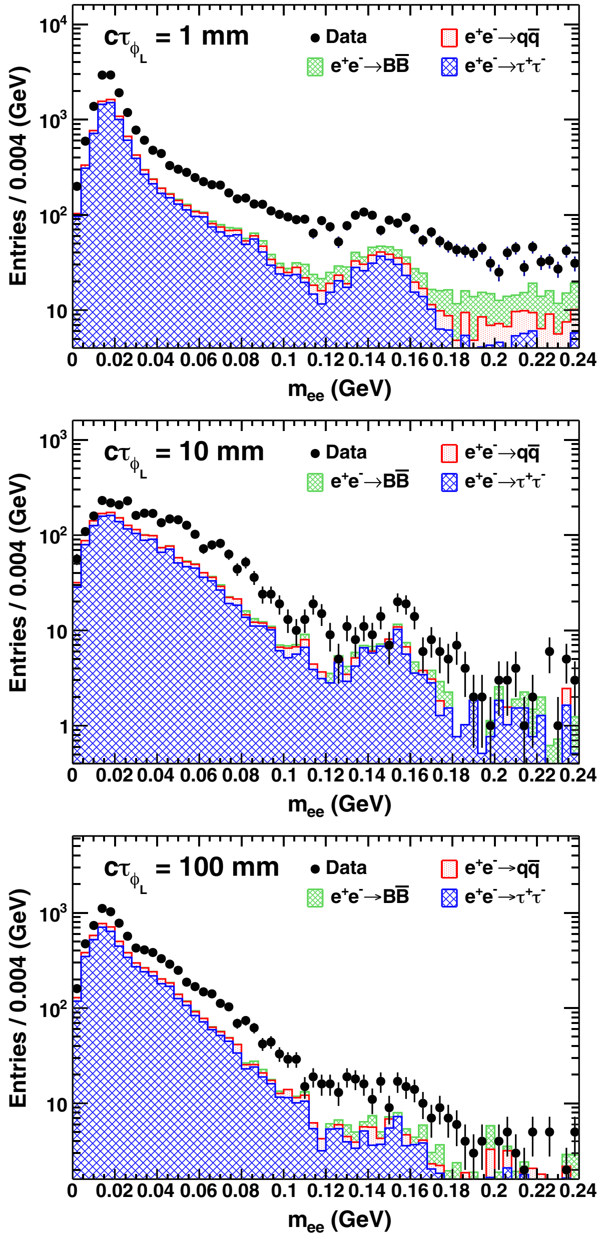

FIG. 2. The distribution of the dielectron invariant mass for the (top) $c\tau_{\phi L} = 1$, (middle) $c\tau_{\phi L} = 10$, and (bottom) $c\tau_{\phi L} = 100$ mm samples, together with simulated predictions for the indicated processes normalized to the integrated luminosity of the data (stacked histograms).

are not simulated, dominated by ISR production of high-multiplicity QED and hadronic events as well as two-photon processes. Peaking contributions from $J/\psi \to \mu^+\mu^-$ and $\psi(2S) \to \mu^+\mu^-$ decays are also seen, and the corresponding regions are excluded from the signal search. In addition, the dielectron spectrum for $c\tau_{\phi L}= 1$ mm features a broad enhancement from $\pi^0 \to \gamma\gamma$ decays in which one or both photons convert to e^+e^- pairs. Since this feature is much broader than the signal, we do not exclude this mass region but instead treat it as an additional background component. No statistically significant π^0 component is observed for other values of $c\tau_{\phi L}$.

We extract the signal yield for the different lifetimes and final states separately by scanning the corresponding mass spectrum in steps of the signal mass resolution, σ. The latter is estimated by performing fits of a double-sided Crystal Ball function [30] to each signal MC sample and interpolating the results to the full mass range. The resolution ranges from 1 MeV near $m_{\phi_L} = 40$ MeV for $c\tau_{\phi L}= 100$ mm to 50 MeV near $m_{\phi_L} = 7.0$ GeV for prompt decays. The signal MC predictions are validated with samples of $K^0_S \to \pi^+\pi^-$ and $\psi(2S) \to \pi^+\pi^- J/\psi$, $J/\psi \to \mu^+\mu^-$ decays; agreement with the data is observed. For each mass hypothesis, we perform an unbinned likelihood fit over an interval varying between $20 - 50\sigma$ (fixed to 60σ) for the dielectron (dimuon) final state. To facilitate the background description, the reduced dimuon mass, $m_R = (m^2_{\mu\mu} - 4m^2_\mu)^{1/2}$, is used for $2m_\mu < m_{\phi_L} < 260\,\mathrm{MeV}$. In that region, fits are performed over a fixed interval $m_R < 0.2$ GeV.

The likelihood function includes contributions from signal, continuum background, and, where needed, peaking components describing the π^0, $J/\psi \to \mu^+\mu^-$, and $\psi(2S) \to \mu^+\mu^-$ resonances. The signal probability density function (pdf) is described by a nonparametric kernel density function modeled directly from the signal MC mass distribution. An algorithm based on the cumulative density function [31] is used to interpolate the pdf between simulated mass points. The uncertainty associated with this procedure is on average 4% (3%) of the corresponding statistical uncertainty for the dielectron (dimuon) analysis.

The dielectron continuum background is modeled by a second-order polynomial for the $c\tau_{\phi L}= 100$ mm sample and by a second-order polynomial plus an exponential function for the other lifetimes. The peaking π^0 shape for the $c\tau_{\phi L}= 1$ mm sample is determined from sideband data obtained by applying all selection criteria, but requiring the χ^2/n.d.f. of the kinematic fit to be greater than 3. The peaking π^0 yield and all the continuum background parameters are determined in the fit. To assess systematic uncertainties, we repeat the fits with a third-order polynomial for the continuum background, vary the width of the π^0 shape within its uncertainty, or include a π^0 component for all lifetime samples. The resulting systematic uncertainties are typically at the level of the statistical uncertainty, but dominate the total uncertainty for several mass hypotheses in the vicinity of the π^0 peak.

The reduced mass distribution of the dimuon continuum background is modeled by a third-order polynomial constrained to intersect the origin, and the dimuon continuum is described by a second-order polynomial at higher masses. The shape of the J/ψ and $\psi(2S)$ resonances are fixed to the predictions of the corresponding MC samples, but their yields cannot be accurately estimated from MC simulations and are therefore left to float freely in the fit. A range of ± 50 MeV around the nominal J/ψ and $\psi(2S)$ masses is therefore excluded from the search. The systematic uncertainty associated with the choice of the background model, assessed by repeating the fits with alternative descriptions, is typically at the level of a few events, but can be as large as half the statistical uncertainty for a few points in the high mass region, where statistical precision is limited.

The fitted signal yields and statistical significances are presented in the Supplemental Material [29], together with a few examples of fits. The bias in the fitted values is determined from pseudoexperiments to be negligible compared to the statistical uncertainties. Since the systematic uncertainty associated with the choice of background model can be large in the dielectron channel, we define the signal significance as the smallest of the significance values determined from each background model. Including trial factors, the largest significance is 1.4σ observed near $m_{\phi_L} = 2.14$ GeV, consistent with the null hypothesis.

The signal efficiency varies between 0.2% for $m_{\phi_L} = 40$ MeV and $c\tau_{\phi L} = 100$ mm, to 26% around $m_{\phi_L} = 5$ GeV for prompt decays. The effect of ISR, not included in the samples generated by MADGRAPH, is assessed by simulating events with PYTHIA8 using the matrix elements calculated by MADGRAPH, and reweighting this sample to match the p_T distribution of the ϕ_L predicted by MADGRAPH. The resulting change in efficiency is found to be about 4% over the full mass range covered by the dielectron channel, and varies from 7% near the dimuon threshold to less than 1% at $m_{\phi_L} \sim 7$ GeV. Half the value of each of these differences is propagated as a systematic uncertainty in the signal yield. A correction factor of 0.98 (0.93) on the signal efficiency is included for the dielectron (dimuon) final state to account for differences between data and simulation in track and neutral reconstruction efficiencies, charged particle identification, and trigger efficiencies. The correction for the dielectron channel is derived from a sample of $K_S^0 \to \pi^+\pi^-$ produced in τ decays, while that for the dimuon channel is assessed from the BDT score distribution for events in which the missing transverse momentum is greater than 2 GeV, a region where the contribution of unsimulated background components can be neglected. An uncertainty of 3.8% (4.0%) in the dielectron (dimuon) efficiency correction is propagated as a systematic uncertainty.

The $e^+e^- \to \tau^+\tau^-\phi_L$ cross section at the $\Upsilon(4S)$ energy is derived for each lifetime and final state by taking into account the variation of the cross section and signal efficiencies with the beam energy and the $\phi_L \to \ell^+\ell^-$ branching fraction:

$$\sigma_{4S} = \frac{N_{\rm sig}}{\sum_{i=2S,3S,4S}(\frac{\sigma_{{\rm th},i}}{\sigma_{th,4S}}\epsilon_i\mathcal{L}_i)BF(\phi_L \to \ell^+\ell^-)},$$

where $N_{\rm sig}$ denotes the number of signal events, and $\sigma_{{\rm th},nS}$, ϵ_{nS} and $\mathcal{L}_{nS}$ ($n = 2$, 3, 4) are the theoretical $e^+e^- \to \tau^+\tau^-\phi_L$ cross section, signal efficiency, and data luminosity at the $\Upsilon(nS)$ center-of-mass energy, respectively. In the absence of a significant signal, Bayesian upper limits at 90% confidence level (CL) on the cross sections are derived by assuming a uniform prior in the cross section. Systematic effects are taken into account by convolving the likelihood with a Gaussian having a width equal to the systematic uncertainty. The uncertainties due to the luminosity (0.6%) [15] and the limited statistical precision of the signal MC sample (1%–4%) are incorporated. The resulting limits are shown in Fig. 3. The sharp increase just above the ditau threshold is a reflection of the $\phi_L \to \mu^+\mu^-$ branching fraction decreasing quickly in favor of the $\tau^+\tau^-$ final state. The limit on the production cross section of a scalar S without any assumptions on other decay modes is presented in the Supplemental Material [29].

The limits on the scalar coupling ξ, presented in Fig. 4, are derived with an iterative procedure that accounts for a potentially long ϕ_L lifetime. An estimate of ξ is first

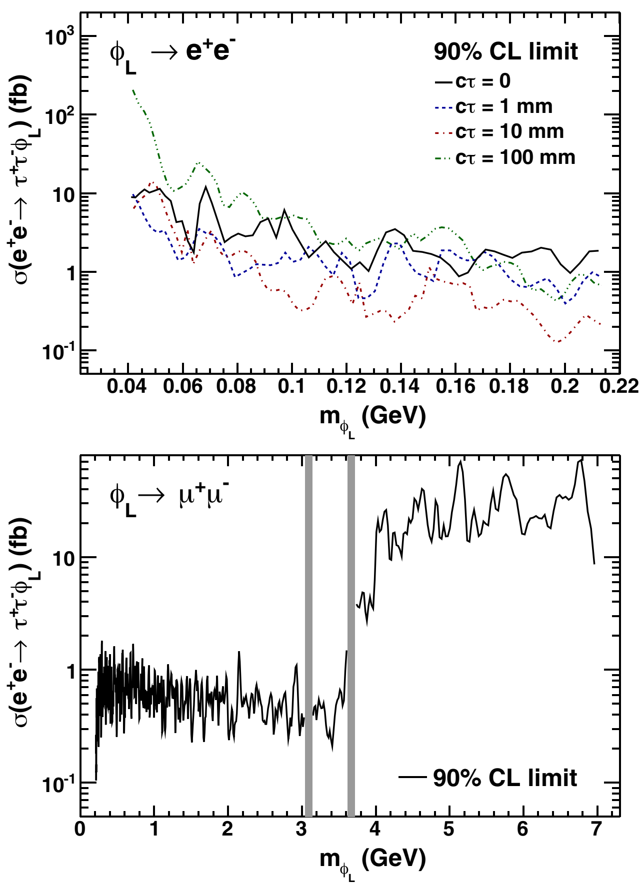

FIG. 3. The 90% C.L. upper limits on the $\sigma(e^+e^- \to \tau^+\tau^-\phi_L)$ cross section at the $\Upsilon(4S)$ resonance derived from (top) the dielectron and (bottom) dimuon final states. The gray bands indicate the regions excluded from the search around the nominal J/ψ and $\psi(2S)$ masses.

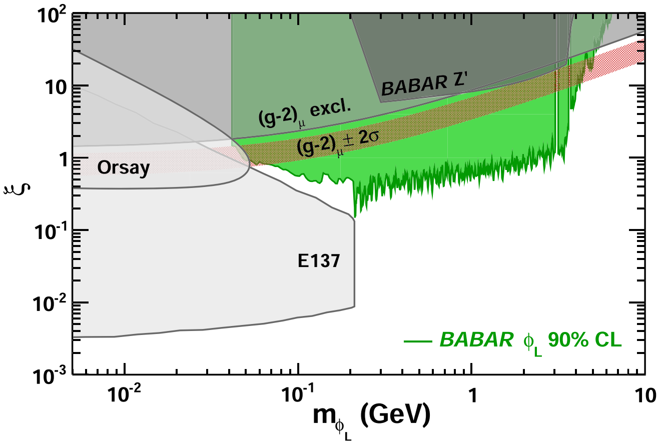

FIG. 4. The 90% C.L. limits on the coupling ξ as a function of the ϕ_L mass (green shaded area), together with existing constraints [9,10,12–14] (gray shaded areas) and the parameter space preferred by the muon anomalous magnetic moment [3,10] (red band).

chosen, and the corresponding lifetime and cross section are calculated [3]. These values are compared to the cross section limit interpolated at that lifetime, and the estimate of the coupling is updated. The procedure is iterated until convergence is obtained. Bounds at the level of 0.5–1 are set on the dielectron final state, corresponding to $c\tau_{\phi L}$ values of the order of 1 cm, and limits down to 0.2 are derived for dimuon decays. These results are approximately an order of magnitude smaller than the couplings favored by the muon anomalous magnetic moment below the ditau threshold [3] and rule out a substantial fraction of previously unexplored parameter space at 90% C.L.

In summary, we report the first model-independent search for the direct production of a new dark leptophilic scalar. The limits significantly improve upon the previous constraints over a large range of masses, almost entirely ruling out the remaining region of parameter space below the dimuon threshold. More significantly, this search excludes the possibility of the dark leptophilic scalar accounting for the observed discrepancy in the muon magnetic moment for almost all ϕ_L masses below 4 GeV. Since these results rely only on ϕ_L production in association with tau leptons and its subsequent leptonic decay, they can also be reinterpreted to provide powerful constraints on other leptonically decaying new bosons interacting with tau leptons. The Belle II experiment should be able to further probe these possibilities, and cover the remaining parameter space above the beam dump constraints.

We are grateful for the extraordinary contributions of our PEP-II colleagues in achieving the excellent luminosity and machine conditions that have made this work possible. The success of this project also relies critically on the expertise and dedication of the computing organizations that support *BABAR*. The collaborating institutions wish to thank SLAC for its support and the kind hospitality extended to them. This work is supported by the U.S. Department of Energy and National Science Foundation, the Natural Sciences and Engineering Research Council (Canada), the Commissariat à l'Energie Atomique and Institut National de Physique Nucléaire et de Physique des Particules (France), the Bundesministerium für Bildung und Forschung and Deutsche Forschungsgemeinschaft (Germany), the Istituto Nazionale di Fisica Nucleare (Italy), the Foundation for Fundamental Research on Matter (Netherlands), the Research Council of Norway, the Ministry of Education and Science of the Russian Federation, Ministerio de Economía y Competitividad (Spain), the Science and Technology Facilities Council (United Kingdom), and the Binational Science Foundation (U.S.-Israel). Individuals have received support from the Marie-Curie IEF program (European Union) and the A. P. Sloan Foundation (USA).

[*]Deceased.
[†]Present address: Wuhan University, Wuhan 430072, China.
[‡]Present address: Università di Bologna and INFN Sezione di Bologna, I-47921 Rimini, Italy.
[§]Present address: King's College, London WC2R 2LS, United Kingdom.
[‖]Present address: University of Huddersfield, Huddersfield HD1 3DH, United Kingdom.
[¶]Present address: University of South Alabama, Mobile, Alabama 36688, USA.
[**]Also at Università di Sassari, I-07100 Sassari, Italy.
[††]Also at Gran Sasso Science Institute, I-67100 LAquila, Italy.

[1] G. C. Branco, P. M. Ferreira, L. Lavoura, M. N. Rebelo, M. Sher, and J. P. Silva, Phys. Rep. **516**, 1 (2012).
[2] B. A. Dobrescu and K. T. Matchev, J. High Energy Phys. 09 (2000) 031.
[3] B. Batell, N. Lange, D. McKeen, M. Pospelov, and A. Ritz, Phys. Rev. D **95**, 075003 (2017).
[4] C. Y. Chen, H. Davoudiasl, W. J. Marciano, and C. Zhang, Phys. Rev. D **93**, 035006 (2016).
[5] J. P. Leveille, Nucl. Phys. **B137**, 63 (1978).
[6] G. W. Bennett *et al.* (Muon g-2 Collaboration), Phys. Rev. D **73**, 072003 (2006).
[7] M. Tanabashi *et al.* (Particle Data Group), Phys. Rev. D **98**, 030001 (2018).
[8] J. Beacham *et al.*, J. Phys. G **47**, 010501 (2020).
[9] Y. S. Liu, D. McKeen, and G. A. Miller, Phys. Rev. Lett. **117**, 101801 (2016).
[10] J. Liu, N. McGinnis, C. E. M. Wagner, and X. P. Wang, J. High Energy Phys. 04 (**2020**) 197.
[11] Natural units ($\hbar = c = 1$) are used throughout this Letter.
[12] J. P. Lees *et al.* (*BABAR* Collaboration), Phys. Rev. D **94**, 011102 (2016).
[13] J. D. Bjorken, S. Ecklund, W. R. Nelson, A. Abashian, C. Church, B. Lu, L. W. Mo, T. A. Nunamaker, and P. Rassmann, Phys. Rev. D **38**, 3375 (1988).

[14] M. Davier and H. Nguyen Ngoc, Phys. Lett. B **229**, 150 (1989).

[15] J. P. Lees *et al.* (*BABAR* Collaboration), Nucl. Instrum. Methods Phys. Res., Sect. A **726**, 203 (2013).

[16] B. Aubert *et al.* (*BABAR* Collaboration), Nucl. Instrum. Methods Phys. Res., Sect. A **479**, 1 (2002).

[17] B. Aubert *et al.* (*BABAR* Collaboration), Nucl. Instrum. Methods Phys. Res., Sect. A **729**, 615 (2013).

[18] J. Alwall, R. Frederix, S. Frixione, V. Hirschi, F. Maltoni, O. Mattelaer, H.-S. Shao, T. Stelzer, P. Torrielli, and M. Zaro, J. High Energy Phys. 07 (**2014**) 079.

[19] T. Sjöstrand, S. Ask, J. R. Christiansen, R. Corke, N. Desai, P. Ilten, S.Mrenna, S. Prestel, C. O. Rasmussen, and P. Z. Skands, Comput. Phys. Commun. **191**, 159 (2015).

[20] S. Jadach, W. Placzek, and B. F. L. Ward, Phys. Lett. B **390**, 298 (1997).

[21] S. Jadach, B. F. L. Ward, and Z. Was, Phys. Rev. D **63**, 113009 (2001).

[22] S. Jadach, Z. Was, R. Decker, and J. H. Kühn, Comput. Phys. Commun. **76**, 361 (1993).

[23] T. Sjöstrand, Comput. Phys. Commun. **82**, 74 (1994).

[24] D. J. Lange, Nucl. Instrum. Methods Phys. Res., Sect. A **462**, 152 (2001).

[25] A. B. Arbuzov, E. A. Kuraev, G. V. Fedotovich, N. P. Merenkov, V. D. Rushai, and L. Trentadue, J. High Energy Phys. 10 (1997) 001.

[26] M. Caffo, H. Czyż, and E. Remiddi, Nuovo Cimento A **110**, 515 (1997); Phys. Lett. B **327**, 369 (1994).

[27] S. Agostinelli *et al.* (GEANT4 Collaboration), Nucl. Instrum. Methods Phys. Res., Sect. A **506**, 250 (2003).

[28] Y. Freund and R. E. Schapire, J. Comput. Syst. Sci. **55**, 119 (1997).

[29] See Supplemental Material at http://link.aps.org/supplemental/10.1103/PhysRevLett.125.181801 for additional plots and a complete description of the variables used for the boosted decision trees.

[30] T. Skwarnicki, Ph.D thesis, DESY F31-86-02, Appendix E, 1986.

[31] A. L. Read, Nucl. Instrum. Methods Phys. Res., Sect. A **425**, 357 (1999).